JAERI-Tech
98-057

DEVELOPMENT OF STEADY STATE MAGNETIC SENSOR

December 1998

Shigemitsu HARA*, Akira NAGASHIMA*
Takahide NAKAYAMA* and Satoshi KASAI

日本原子力研究所
Japan Atomic Energy Research Institute

本レポートは，日本原子力研究所が不定期に公刊している研究報告書です。
入手の問合わせは，日本原子力研究所研究情報部研究情報課（〒319－1195 茨城県那珂郡東海村）あて，お申し越しください。なお，このほかに財団法人原子力弘済会資料センター（〒319－1195 茨城県那珂郡東海村日本原子力研究所内）で複写による実費頒布をおこなっております。

This report is issued irregularly.
Inquiries about availability of the reports should be addressed to Research Information Division, Department of Intellectual Resources, Japan Atomic Energy Research Institute, Tokai-mura, Naka-gun, Ibaraki-ken 〒319－1195, Japan.

編集兼発行　日本原子力研究所

Development of Steady State Magnetic Sensor

Shigemitsu HARA*, Akira NAGASHIMA+, Takahide NAKAYAMA*
and Satoshi KASAI

Department of Fusion Engineering Research
Naka Fusion Research Establishment
Japan Atomic Energy Research Institute
Naka-machi, Naka-gun, Ibaraki-ken

(Received November 18 ,1998)

A prototype of new mechanical sensor based on the steady state electromagnetic force (J × B force) measurement has been developed and tested. The mechanical force sensor is a new type of the magnetic sensor which is available for frequencies smaller than 0.1Hz. The prototype of the mechanical sensor has been examined, and the following results were obtained;

(1) A signal was proportional to simulated force in the load cell tests.

(2) A signal drift concerning the temperature was reproducible over the range of the ITER environment.

(3) A signal was proportional to the magnetic field in the steady state magnetic field measurement tests.

(4) A load cell linearity error did not increase significantly after irradiation of 7.2 × 10^6Gy.

These results indicate that the mechanical sensor will provide the practical feasibility in the long time magnetic field measurement.

Keywords : Steady State Magnetic Sensor, ITER, Irradiation Test, Load Cell, Diagnostics

This R&D work was carried out under the ITER EDA task agreement of R&D task (Task agreement number : S55 TT 13 97-10-24 FJ, Task number : T347 FJ-4) .

+ Advanced photon Research Center Kansai Research Establishment

* Hitachi, Ltd.

定常磁場センサーの開発

日本原子力研究所那珂研究所核融合工学部
原　重充*・長島　章+・中山　尚英*・河西　敏

(1998年11月18日受理)

核融合実験炉（ITER）の長時間放電や定常放電において、定常磁場を計測できるローレンツカ（J×B）の計測に基づくセンサーの開発を行い、特性試験を実施した。このセンサーは、0.1Hz以下の低周波磁場を検出するため磁場感知コイルとロードセルから構成されたメカニカルセンサーと通常の磁気プローブから構成されている。最も重要な開発要素であるメカニカルセンサーについてプロトタイプを製作し、その性能試験を行い、以下のような結果を得た。

(1)ロードセルの試験で、加えた力に比例した信号が得られた。

(2) ITERにおける使用温度領域で、温度によりセンサーの出力信号がドリフトするが、再現性のあることがわかった。

(3)センサーに定常磁場を加えた試験で、センサーの出力信号は磁場に対して再現性のあることがわかった。

(4) 7.2×10^6Gyまでのガンマ線を照射した後でも、ロードセル出力の直線性に対する誤差が顕著に増大しないことがわかった。

本開発は、ITER工学R＆Dの一環として行ったものであり、R＆Dタスク（Task agreement number：S55TT13　97-10-24 FJ、Task ID number：T 347 FJ-4）に基づくものである。

那珂研究所：〒311-0193　茨城県那珂郡那珂町向山801-1
＋関西研究所光量子科学センター
＊㈱日立

Contents

目　　次

1. Introduction

Measurement of magnetic field under quasi-steady state is important for long pulse operation on ITER. Present inductive methods have a limit of time integration in the range over several thousand seconds. A new concept of a hybrid magnetic sensor has been proposed to execute measurement of steady state magnetic field[1,2,3]. This new sensor is based on a combination of a conventional magnetic probe for the measurement of high frequency magnetic field and a mechanical sensor[1,3,4] or a rotating magnetic probe[2,5] for that of low frequency magnetic field. The rotating probe employs a drive mechanism by a high speed air turbine and is not used any mechanical contacts to pick up the electric signal induced in the rotating probe. In order to attain the accuracy of magnetic field measurement, it is necessary to keep the air pressure constant in the air turbine as possible. The mechanical sensor, which consist of a sensing coil and a load cell, employs the measurement of an electromagnetic force. The force induced on the sensing coil is detected by the load cell which mechanically connects with the sensing coil. Details of principle and mechanism are described in the Refs. 3 and 4. In order to demonstrate the hybrid sensor experimentally, functional tests, i.e. evaluation of drift and response, and long time measurement tests were carried out using the JT-60U Tokamak discharges[3,4]. It was found that the hybrid sensor can measure real magnetic field essentially[3,4].

In the application of this sensor to ITER, it is necessary to develop the radiation hardened sensor and the key component of development is mainly included in the mechanical sensor part. The objective of the R&D is to fabricate a prototype mechanical sensor and to examine the capability of the sensor performance including examination for the performance preservation before and after irradiation of strong gamma-ray field.

2. Technical Outline

2.1. Item of R&D

(1) Design of a prototype hybrid magnetic sensor
(2) Fabrication of the sensor
(3) Study of the sensitivity of the sensor

2.2. Item of Test

(1) Pre-irradiation sensitivity test	: Accuracy, Drift, Range
(2) Irradiation test	: 10^4 Gy/h×1 month
(3) Post-irradiation sensitivity test	: Accuracy, Drift, Range

3. Design and Fabrication of a Prototype Mechanical Sensor

A prototype mechanical sensor has been designed, which consists of the sensing coil/frame, sensing coil support, a load cell and a sensor base plate. Figure 1 shows the structure of the mechanical sensor. The sensing coil is designed by considering that electromagnetic force on the sensing coil should be strong enough to be detected by the load cell. This coil is made of the copper wire coated with polyimide insulator and the wire is wound by 60 turns on the sensing coil frame made of aluminum. The length and width of the sensing

coil are 157 mm and 50 mm, respectively. The sensing coil is supported by thin phosphor bronze plates on the both side of the load cell as shown in Fig. 1. In this coil, the constant current is supplied externally. The coil can be rotated slightly around the supporting plate when the magnetic field is supplied on the coil. Also, the sensing coil/frame connects with the load cell by the sensor beam in order to conduct the mechanical force, i.e. torque of the coil to the load cell. The material of the joint between the frame and beam is thin phosphor plate. This structure relieves the thermal expansion of the sensing coil/frame, which causes the noise. The load cell consists of a strain gauge made of a constantan wire and a beryllium copper beam. The couple of strain gauge are bonded on the beam by phenol in order to detect the strain in the independent two directions. In this design, the force is estimated to be 2.45 gf with the sensing coil current of 0.5 A in the magnetic field of 100 Gauss. Figure 2 shows the fabricated prototype mechanical sensor. The material of sensor base plate is 304 stainless steel. Figure 3 shows an equivalent circuit of the mechanical sensor.

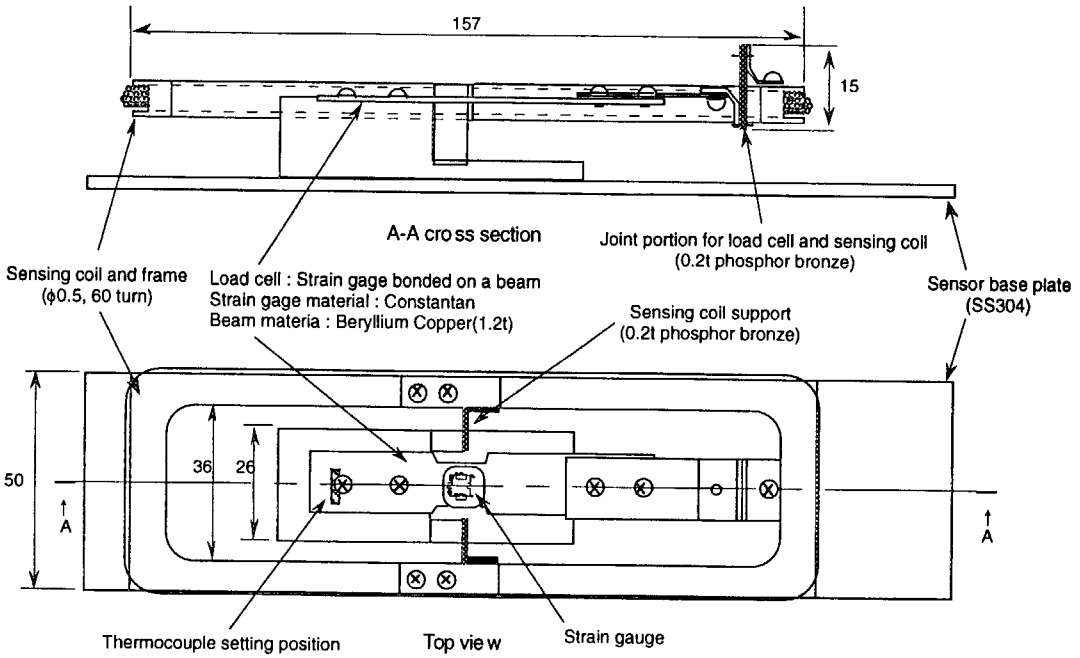

Fig. 1 The structure of mechanical sensor.

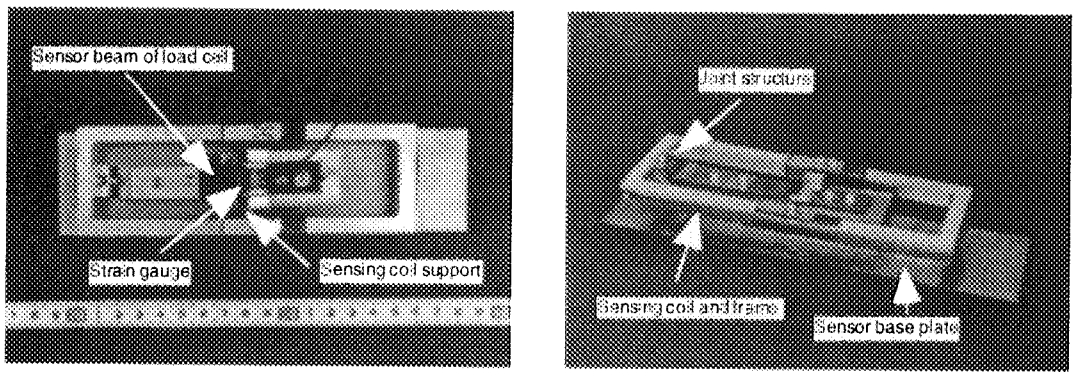

(a) Top view (b) Side view

Fig. 2 Fabricated mechanical sensor.

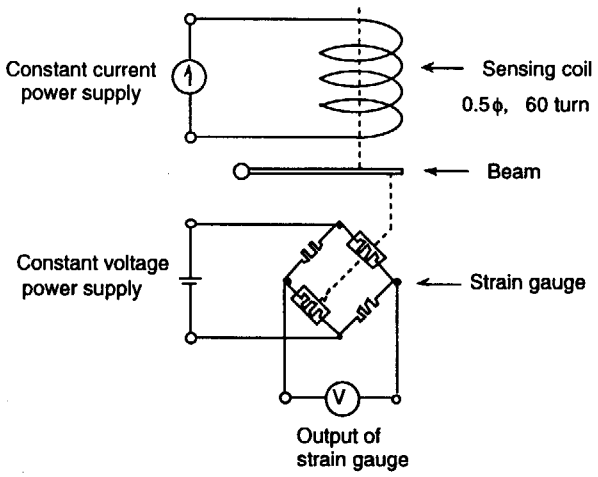

Fig. 3 Equivalent circuit of mechanical sensor.

The strain gauge forms an electrical bridge circuit. When electromagnetic force is applied to the sensing coil, the output of the bridge circuit is expected to be proportional to the electromagnetic force.

4. Pre-Irradiation Tests

4.1 Sensitivity test

Feasibility of the prototype mechanical sensor has been examined concerning to the stability of the load cell sensitivity. Figure 4 shows the block diagram of a testing apparatus to examine the sensitivity performance on the high temperature. The temperature of the sensor is raised up to 240 °C by the electrical sheath heater. Known weight of 1, 2×2, 5, 2×10, 20, 50, 100, 200 g were used for the sensitivity examination of the sensor (load cell). The temperature of mechanical sensor is monitored and controlled during the test. The load cell signal was obtained as an output signal of a commercially available strain

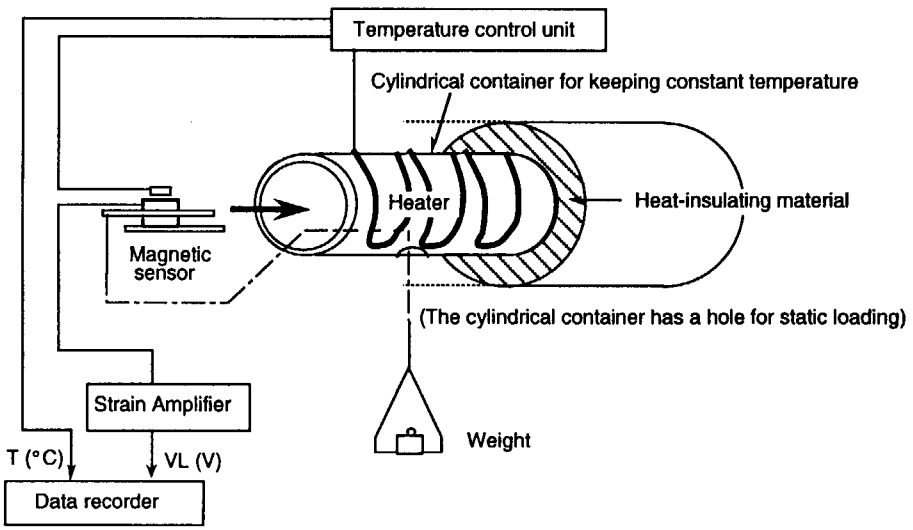

Fig. 4 Block diagram of a high temperature sensitivity testing apparatus.

amplifier module (DPM-700B: Kyowa Electronic Instruments Ltd.). The gauge of temperature and weight were recorded by the data acquisition system.

The load cell sensitivity as a function of the temperature is shown in Fig. 5. The data were plotted at temperatures of 24, 50, 100, 150, 200 and 240 °C, whose temperatures were measured by the thermocouple at the position of the load cell as shown in Fig.1. The sensitivity was measured two times in each temperature. The first and second measurements are noted by -a and -b in Fig. 5, respectively. The linearity in the sensitivity of the load cell was obtained relating to the applied weights. In the results, thermal offset drift was observed. Figure 6 shows the load cell sensitivity as a function of the decreasing temperature from 240 °C to 24 °C . The first and second measurements are noted by -c and -d in this figure, respectively. In this case, the sensitivity behavior is similar to the temperature ramp-up case.

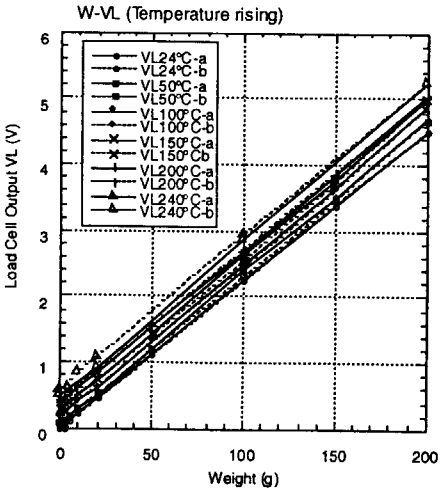

Fig. 5 The load cell sensitivity test result related to temperature and applied weight (Temperature rising).

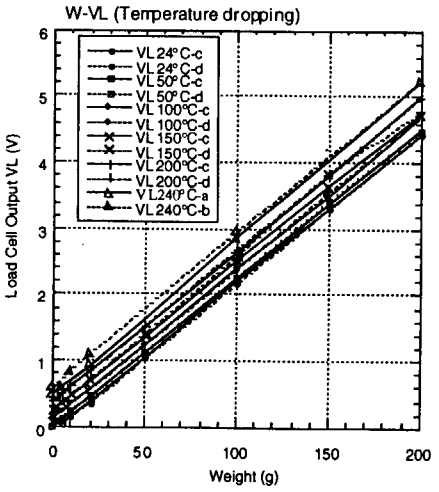

Fig. 6 The load cell output sensitivity test result related to temperature and applied weight (Temperature dropping).

Figure 7 shows the dependence of the zero-level drift on the temperature. The zero-level drift is proportional to the temperature. In this figure, the Vfit line was obtained by using the least square fitting. A slight non-linearity was observed which may cause measurement error within 0.1 V. This error is evaluated to be 2% for the maximum output signal of 5.2 V. However, the zero-level drift is not a severe problem for the actual measurements because we can correct the drift from the reproducibility. Further, the drift can be measured by breaking the sensing coil current.

Figure 8 shows the dependence of the differential sensitivity (VL/W) on the temperature. The deviation of the differential sensitivity data from a fitting line Vfit means a disagreement from the precise linearity. The Vfit line was obtained by using the least square fitting. There was the non-linearity of the differential sensitivity (VL/W) relating to the temperature. The deviation of the data from the fitting line is smaller than 0.0006 V/g. The error corresponds to 2.5% for the gradient range of 0.0236 V/g.

4.2 Magnetic field measurement test

The examination to measure the magnetic field has been carried out

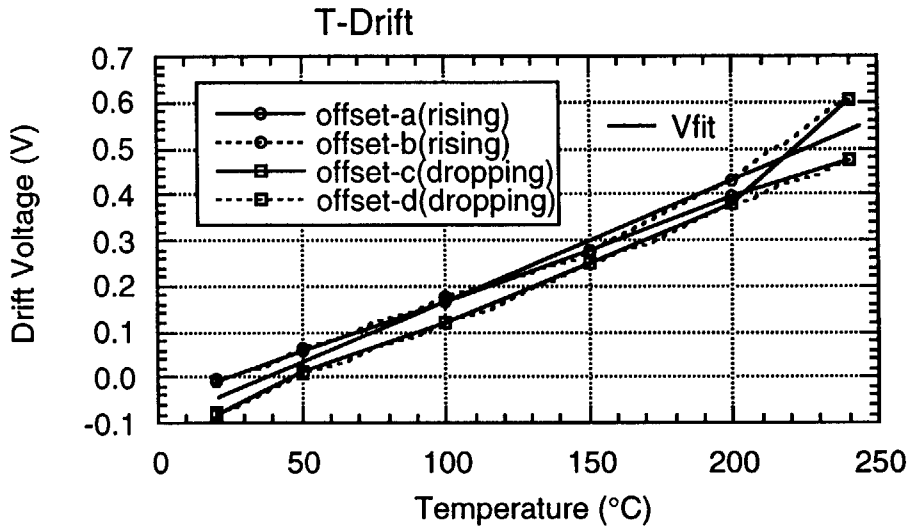

Fig. 7 The dependence of the zero-level drift on temperature.

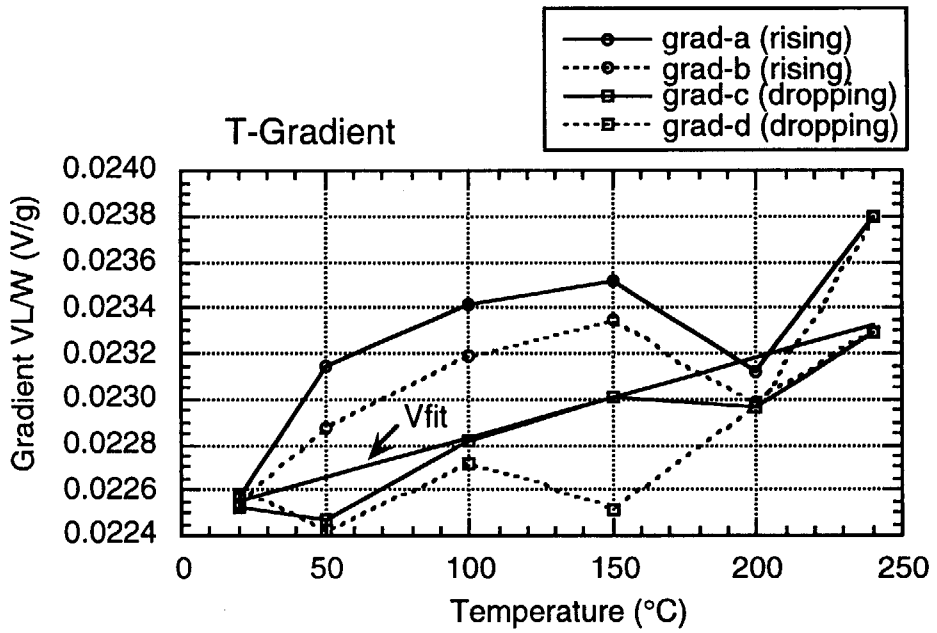

Fig. 8 The dependence of the gradient VL/W on temperature.

using the steady state magnetic field generator in NAKA/ JAERI. Figure 9 shows the block diagram of the apparatus for the magnetic measurement test. This apparatus can generate the stationery magnetic field up to 650 G. A Hall element gauss meter is used to calibrate the applied field. The value of the magnetic field is monitored and controlled during the test. The load cell signal was obtained as an output signal of a strain gauge amplifier. The signal data of load cell output VL, magnetic field B and sensing coil current I_S were recorded by a data acquisition system.

Figure 10 shows the applied magnetic field and the load cell signal obtained as the magnetic field was increased up to 650 G. In this figure, the load cell signal multiplied by 517.89 is shown as the mechanical sensor output. The dependence of the load cell output on the magnetic field with the sensing coil current of 0.5 A is shown in Fig.11. The function Vfit described in this figure

was obtained by the least square fitting. The coefficient of $I_S \times B$ indicates the linearity of the load cell output for the magnetic field. A maximum linearity error (e_{max}) is less than 0.1 % between the load cell output and the fitted function Vfit.

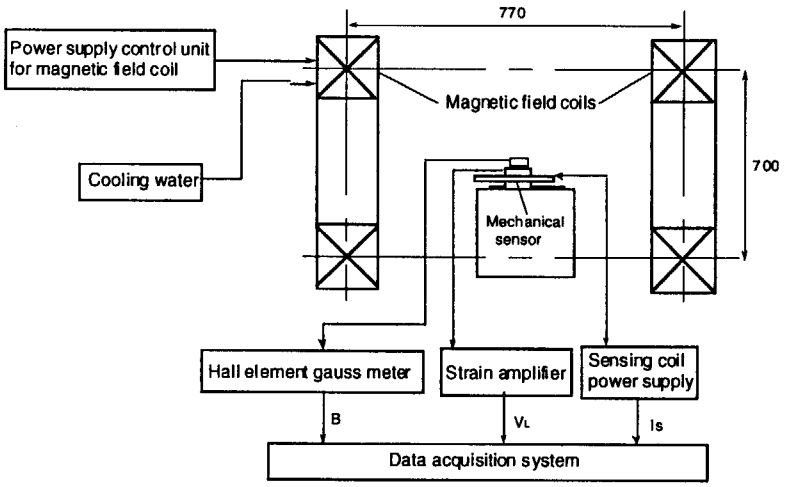

Fig. 9 Block diagram of the magnetic measurement testing apparatus.

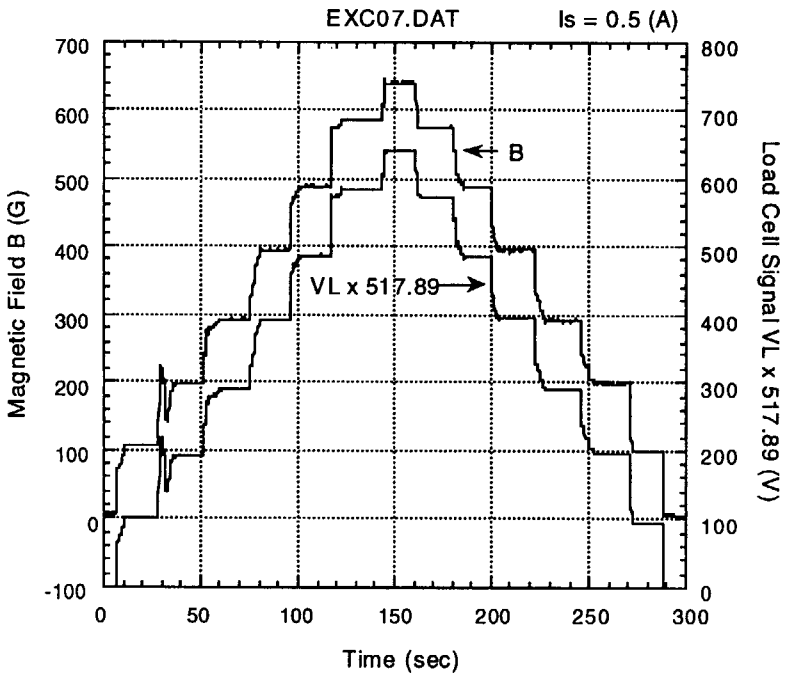

Fig. 10 Wave forms of the load cell output (VL) multiplied by 517.89 and externally applied magnetic field (B) in the steady state magnetic field measurement test.

5. Irradiation Tests

The irradiation effect on the hybrid sensor is one of the most important issues in the development of the steady state magnetic sensor. Especially, RIC (radiation induced conductivity) and RIED (radiation induced electrical

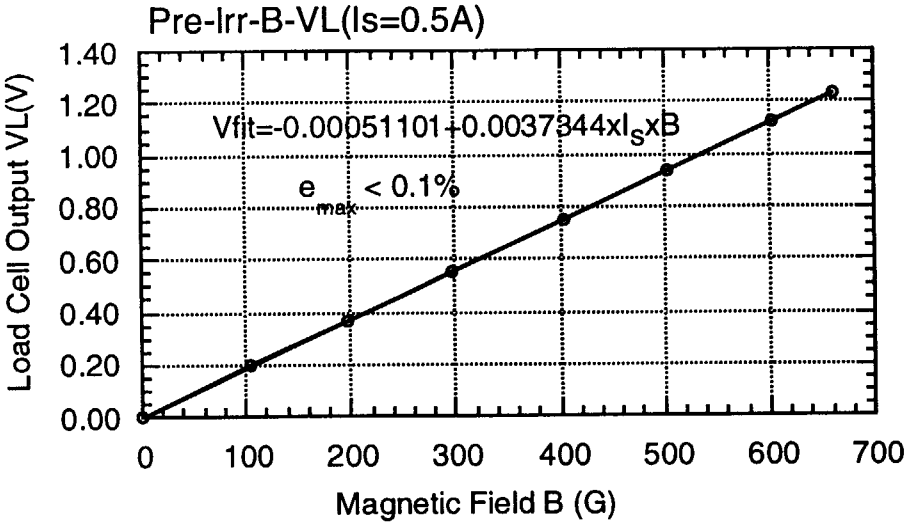

Fig. 11 The dependence of the load cell output on the magnetic field (I_S=0.5 A).

degradation) of insulating materials are anticipated under DC/AC electrical fields.

The performance of the load cell and the sensing coil under gamma irradiation has been investigated using the Co^{60} irradiation facility in JAERI Takasaki. The geometrical arrangement of the gamma irradiation test facility for the mechanical sensor is shown in Fig. 12(a) and the photograph of the chamber for the mechanical sensor is shown in Fig. 12(b). The sensor was installed in the cylindrical chamber with an inner diameter of 60 mm in which was pumped out in order to avoid surface oxidation of the sensor material. The absorbed dose rate of gamma ray is 10^4 Gy/h and the total dose is 7.2×10^6 Gy for 30 days.

6. Post-Irradiation Tests

6.1 Sensitivity test.

The irradiation effect has been examined concerning the degradation of the load cell sensitivity. Figures 13 and 14 show the test results obtained in the increasing phase of the temperature up to 240 °C and the decreasing phase. The data were obtained in the same way with Figs. 5 and 6. The linearity of the sensitivity of the load cell signal was obtained relating to the applied weights. In these cases, thermal offset drift was observed. It was found that there was no significant change in the linearity of the sensitivity before and after irradiation.

Figure 15 shows the dependence of the zero-level drift on the temperature. The zero-level drift was proportional to the temperature with a slight non-linearity. It may cause the measurement error within 0.1 V. This error corresponds to 2% for the maximum output signal of 5 V. Also, there was no difference in the thermal offset drift behavior before and after irradiation.

Figure 16 shows the dependence of the differential sensitivity (VL/W) against the temperature. The deviation of the differential sensitivity data from a fitting line means a disagreement from the precise linearity. The non-linearity in the differential sensitivity (VL/W) was observed for the temperature. It may cause the measurement error within 0.0003 V/g. The load

cell linearity error did not increase after irradiation.

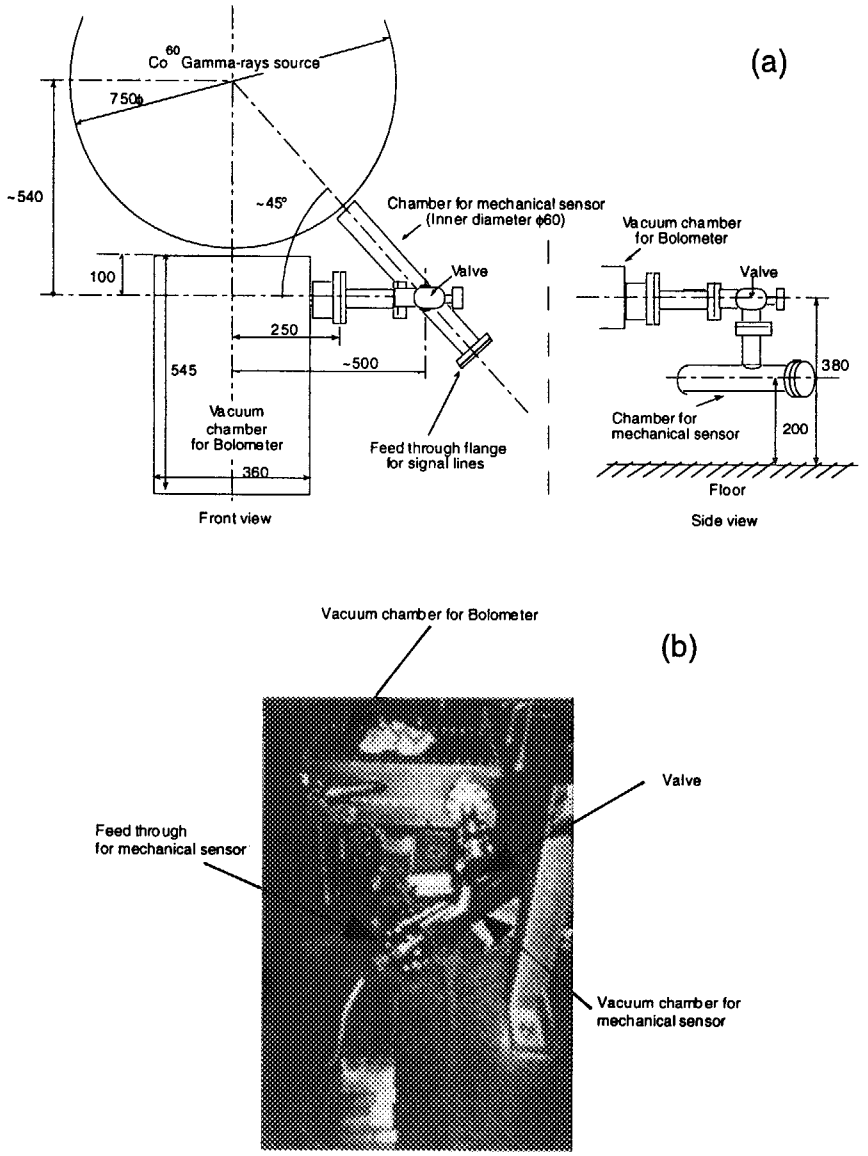

Fig. 12 (a) The gamma irradiation test facility for steady state magnetic sensor, (b) The photograph of the vacuum chamber for the mechanical sensor.

6.2 Magnetic field measurement test

The examination of the magnetic field measurement has been carried out to investigate the irradiation degradation on the load cell sensitivity. Figure 17 shows the change of the load cell signal multiplied by 617.3 when the magnetic field was increasing and decreasing step by step between 0 and 700 G. Figure 18 shows the dependence of the load cell output on the magnetic field with a sensing coil current of 0.5 A. The load cell output was proportional to the magnetic field. This result indicates that the load cell had the linear sensitivity for the applied field. A maximum linearity error (e_{max}) is less than 0.2 % between the output data and the fitted function Vfit. The reduction of electromagnetic force sensitivity after irradiation was about 3 % from the prior

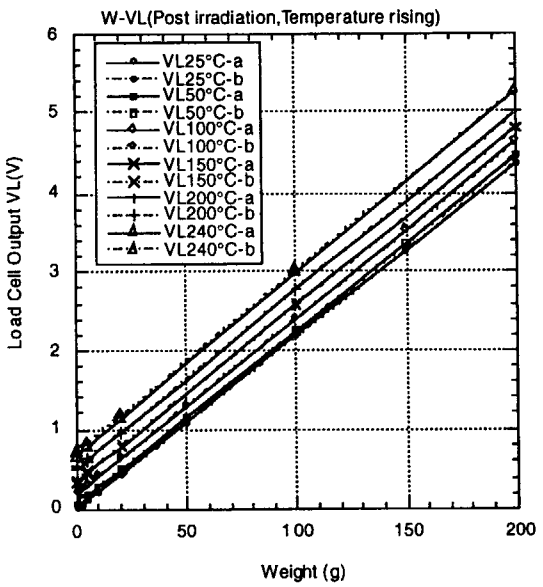

Fig. 13 The load cell output sensitivity test result related to temperature and applied weight (Post irradiation, Temperature rising).

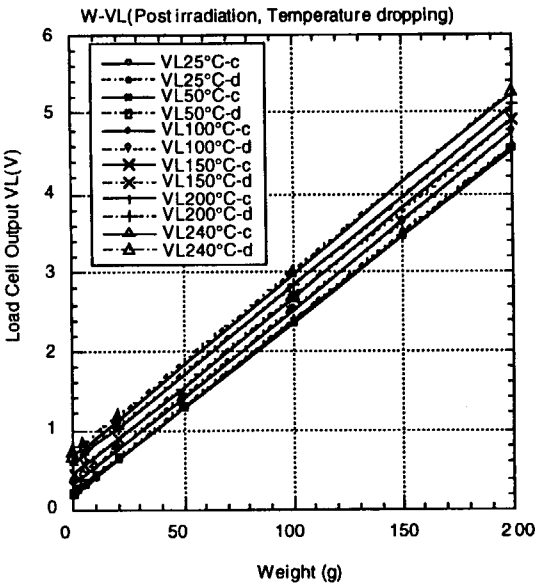

Fig. 14 The load cell output sensitivity test result related to temperature and applied weight (Post irradiation, Temperature dropping).

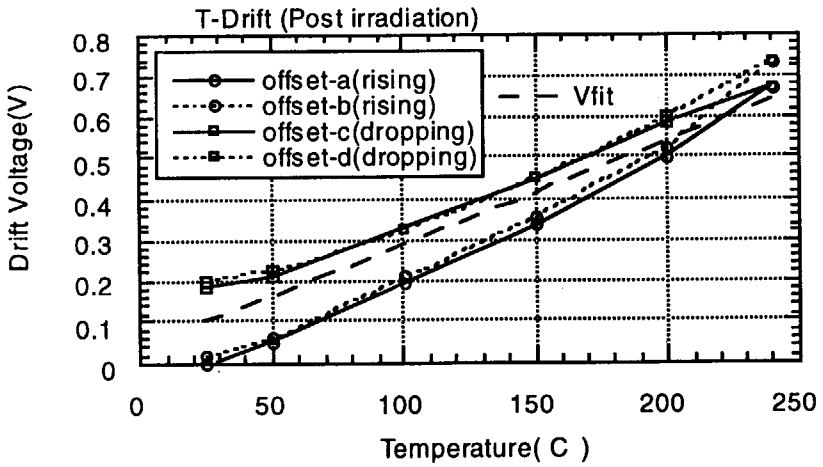

Fig. 15 The dependence of the zero-level drift on temperature (Post irradiation).

sensitivity. However, it is unclear that the reduction was caused either by irradiation effect or by gain adjustment error of the amplifier for load cell and the gauss meter setting error.

Figure 19 shows the dependence of the load cell output on the sensing coil current in the magnetic field of 600 G. The load cell output was proportional to the sensing coil current. A maximum linearity error (e_{max}) is less than 0.2 % between the output data and the fitted function Vfit.

These results show that there was no significant increase in the load cell linearity error after irradiation and the mechanical sensor will provide the practical feasibility in the long time magnetic field measurement.

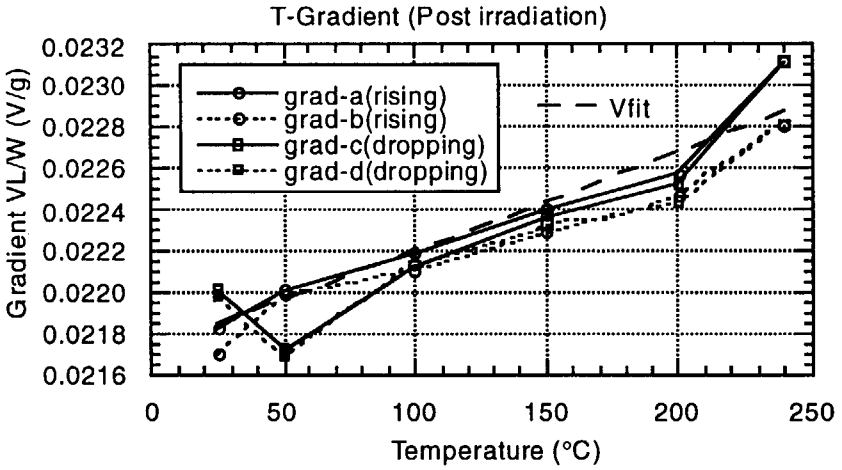

Fig. 16 The dependence of the gradient VL/W on temperature (Post irradiation).

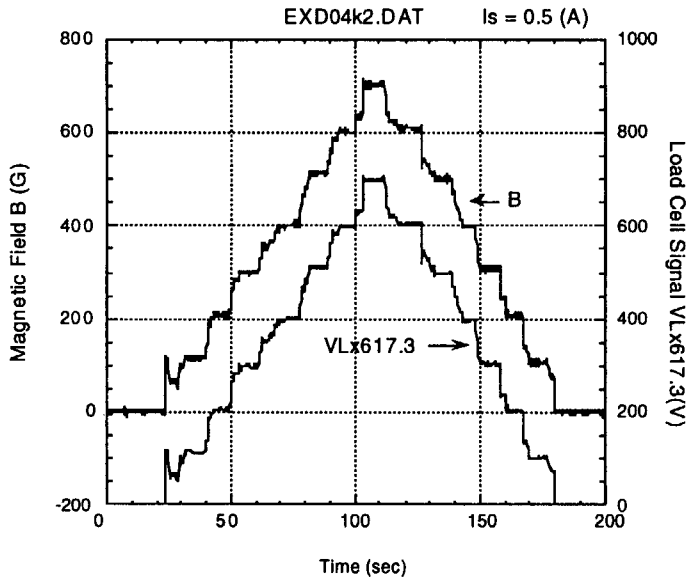

Fig. 17 Wave forms of the load cell output (VL) multiplied by 617.3 and externally applied magnetic field (B) in the steady state magnetic field measurement test (Post irradiation).

7. Conclusions

The prototype of the steady state magnetic sensor employed a new mechanical sensor has been developed. The sensor consists of the sensing coil and the load cell. The characteristics of the mechanical sensor were examined before and after gamma ray irradiation of 7.2×10^6 Gy and the following results were obtained.

(1) The signal was proportional to simulated force in the load tests.
(2) Nearly the reproducible signal drift was proportional to the temperature in the temperature range of 24 to 240 °C.
(3) Residual thermal drift irreproducibility may cause the measurement error of 2 % for the maximum output signal range.
(4) The differential sensitivity VL/W depended on the temperature. The

measurement error may be within 2.5%.

(5) The signal was proportional to the magnetic field linearly in the steady state magnetic field measurement tests. The measurement error is to be less than 0.2 % .

(6) The load cell linearity error did not increase significantly after irradiation of 7.2×10^6 Gy.

These results show that the mechanical sensor will provide the practical feasibility in the long time magnetic field measurement.

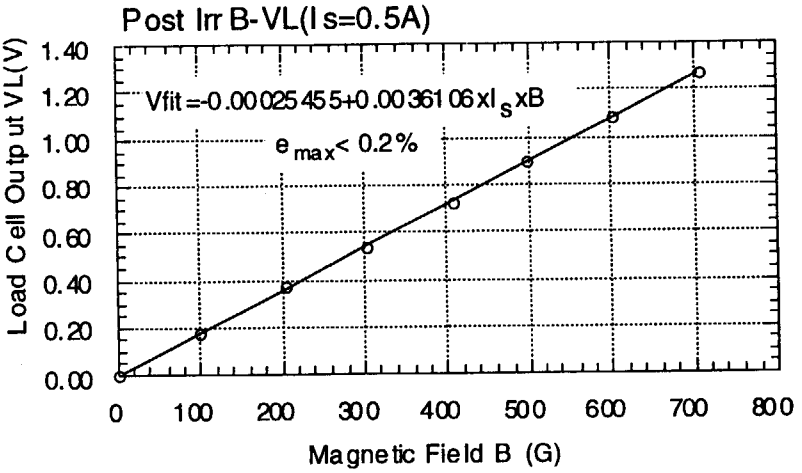

Fig. 18 The dependence of the load cell output on the magnetic field (I_S=0.5A, Post irradiation).

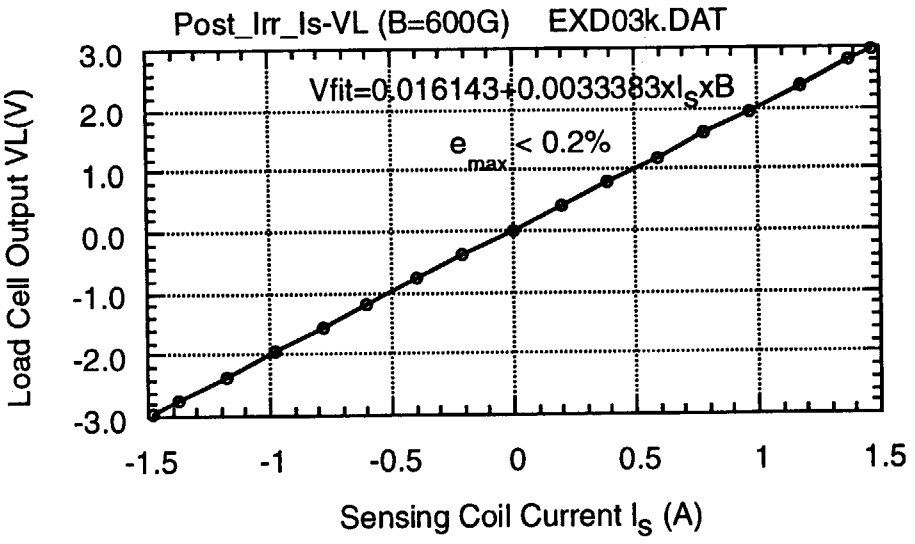

Fig. 19 The dependence of the load cell output on the sensing coil current (B=600 G, Post irradiation).

Acknowledgments

The authors are grateful to Drs. L. deKock, A. Costley and S. Yamamoto for their fruitful discussions and cooperation and to the members of Hitachi

Ltd. for their marvelous manufacturing. This paper has been prepared as an account of work assigned to the Japanese Home Team under Task Agreement number S55 TT 13 97-10-24 FJ within the Agreement among the European Atomic Energy Community, the Government of Japan, the Government of the Russian Federation, and the Government of the United States of America on Cooperation in the Engineering Design Activities for the International Thermonuclear Experimental Reactor ("ITER EDA Agreement") under the auspices of the International Atomic Energy Agency (IAEA).

References

[1] Robert D. Woolley : Tokamak Poloidal Magnetic Field Measurements Accurate for Unlimited Time Duration, 16th IEEE/NPSS Symposium on Fusion Engineering, 1995, vol.2, p1530.
[2] K. Matsuura, M. Sakata, S. Fujiwaka and J. Fujita : Kakuyugo Kenkyu **70** (1994)397.
[3] S. Hara, M. Abe and K. Moriyama : Development of a Magnetic Sensor for Nuclear Fusion Reactor, Proceedings of 12th autumn meeting held at Iwate university in Japan, The Japan Society of Plasma Science and Nuclear Fusion Research, 1995, p85 (in Japanese).
[4] S. Hara, M. Abe and K. Moriyama : Kakuyugo Kenkyu **73** (1997)501-509, S. Hara, Y. Neyatani, M. Abe, A. Nagashima, S. Kasai : in Diagnostic for Experimental Thermonuclear Fusion Reactors, edted by P. E. Stott, G. Gorini and E. Sindoni (Plenum Press, New York, 1998) p525.
[5] K. Kawahata, J. Fujita, K. Matsuura, M. Sakata, S. Fujiwaka, T. Matoba : JAERI-Tech 95-041 (1995).

国際単位系 (SI) と換算表

表 1　SI 基本単位および補助単位

量	名称	記号
長さ	メートル	m
質量	キログラム	kg
時間	秒	s
電流	アンペア	A
熱力学温度	ケルビン	K
物質量	モル	mol
光度	カンデラ	cd
平面角	ラジアン	rad
立体角	ステラジアン	sr

表 2　SI と併用される単位

名称	記号
分，時，日	min，h，d
度，分，秒	°，′，″
リットル	l，L
トン	t
電子ボルト	eV
原子質量単位	u

1 eV = 1.60218 × 10^{-19} J

1 u = 1.66054 × 10^{-27} kg

表 5　SI 接頭語

倍数	接頭語	記号
10^{18}	エクサ	E
10^{15}	ペタ	P
10^{12}	テラ	T
10^{9}	ギガ	G
10^{6}	メガ	M
10^{3}	キロ	k
10^{2}	ヘクト	h
10^{1}	デカ	da
10^{-1}	デシ	d
10^{-2}	センチ	c
10^{-3}	ミリ	m
10^{-6}	マイクロ	μ
10^{-9}	ナノ	n
10^{-12}	ピコ	p
10^{-15}	フェムト	f
10^{-18}	アト	a

表 3　固有の名称をもつ SI 組立単位

量	名称	記号	他の SI 単位による表現
周波数	ヘルツ	Hz	s^{-1}
力	ニュートン	N	$m \cdot kg/s^2$
圧力，応力	パスカル	Pa	N/m^2
エネルギー，仕事，熱量	ジュール	J	N·m
工率，放射束	ワット	W	J/s
電気量，電荷	クーロン	C	A·s
電位，電圧，起電力	ボルト	V	W/A
静電容量	ファラド	F	C/V
電気抵抗	オーム	Ω	V/A
コンダクタンス	ジーメンス	S	A/V
磁束	ウェーバ	Wb	V·s
磁束密度	テスラ	T	Wb/m^2
インダクタンス	ヘンリー	H	Wb/A
セルシウス温度	セルシウス度	℃	
光束	ルーメン	lm	cd·sr
照度	ルクス	lx	lm/m^2
放射能	ベクレル	Bq	s^{-1}
吸収線量	グレイ	Gy	J/kg
線量当量	シーベルト	Sv	J/kg

表 4　SI と共に暫定的に維持される単位

名称	記号
オングストローム	Å
バーン	b
バール	bar
ガル	Gal
キュリー	Ci
レントゲン	R
ラド	rad
レム	rem

1 Å = 0.1 nm = 10^{-10} m

1 b = 100 fm^2 = 10^{-28} m^2

1 bar = 0.1 MPa = 10^5 Pa

1 Gal = 1 cm/s^2 = 10^{-2} m/s^2

1 Ci = 3.7 × 10^{10} Bq

1 R = 2.58 × 10^{-4} C/kg

1 rad = 1 cGy = 10^{-2} Gy

1 rem = 1 cSv = 10^{-2} Sv

（注）

1. 表 1 − 5 は「国際単位系」第 5 版，国際度量衡局 1985 年刊行による。ただし，1 eV および 1 u の値は CODATA の 1986 年推奨値によった。
2. 表 4 には海里，ノット，アール，ヘクタールも含まれているが日常の単位なのでここでは省略した。
3. bar は，JIS では流体の圧力を表わす場合に限り表 2 のカテゴリーに分類されている。
4. EC 閣僚理事会指令では bar，barn および「血圧の単位」mmHg を表 2 のカテゴリーに入れている。

換算表

力	N(=10^5 dyn)	kgf	lbf
	1	0.101972	0.224809
	9.80665	1	2.20462
	4.44822	0.453592	1

粘度　1 Pa·s(N·s/m^2) = 10 P(ポアズ)(g/(cm·s))

動粘度　1 m^2/s = 10^4 St(ストークス)(cm^2/s)

圧力	MPa(=10 bar)	kgf/cm^2	atm	mmHg(Torr)	lbf/in^2(psi)
	1	10.1972	9.86923	7.50062 × 10^3	145.038
	0.0980665	1	0.967841	735.559	14.2233
	0.101325	1.03323	1	760	14.6959
	1.33322 × 10^{-4}	1.35951 × 10^{-3}	1.31579 × 10^{-3}	1	1.93368 × 10^{-2}
	6.89476 × 10^{-3}	7.03070 × 10^{-2}	6.80460 × 10^{-2}	51.7149	1

エネルギー・仕事・熱量	J(=10^7 erg)	kgf·m	kW·h	cal(計量法)	Btu	ft·lbf	eV
	1	0.101972	2.77778 × 10^{-7}	0.238889	9.47813 × 10^{-4}	0.737562	6.24150 × 10^{18}
	9.80665	1	2.72407 × 10^{-6}	2.34270	9.29487 × 10^{-3}	7.23301	6.12082 × 10^{19}
	3.6 × 10^6	3.67098 × 10^5	1	8.59999 × 10^5	3412.13	2.65522 × 10^6	2.24694 × 10^{25}
	4.18605	0.426858	1.16279 × 10^{-6}	1	3.96759 × 10^{-3}	3.08747	2.61272 × 10^{19}
	1055.06	107.586	2.93072 × 10^{-4}	252.042	1	778.172	6.58515 × 10^{21}
	1.35582	0.138255	3.76616 × 10^{-7}	0.323890	1.28506 × 10^{-3}	1	8.46233 × 10^{18}
	1.60218 × 10^{-19}	1.63377 × 10^{-20}	4.45050 × 10^{-26}	3.82743 × 10^{-20}	1.51857 × 10^{-22}	1.18171 × 10^{-19}	1

1 cal = 4.18605 J (計量法)
= 4.184 J (熱化学)
= 4.1855 J (15 °C)
= 4.1868 J (国際蒸気表)

仕事率　1 PS (仏馬力)
= 75 kgf·m/s
= 735.499 W

放射能	Bq	Ci
	1	2.70270 × 10^{-11}
	3.7 × 10^{10}	1

吸収線量	Gy	rad
	1	100
	0.01	1

照射線量	C/kg	R
	1	3876
	2.58 × 10^{-4}	1

線量当量	Sv	rem
	1	100
	0.01	1

（86 年 12 月 26 日現在）

DEVELOPMENT OF STEADY STATE MAGNETIC SENSOR